Putative dendritic correlates of chronic traumatic encephalopathy: A preliminary quantitative Golgi exploration

Allysa Warling[1], **Riri Uchida**[1], **Hyunsoo Shin**[1], **Coby Dodelson**[1], **Madeleine E. Garcia**[1], **N. Beckett Shea-Shumsky**[1], **Sarah Svirsky**[2], **Morgan Pothast**[2], **Hunter Kelley**[2], **Cynthia M. Schumann**[3], **Christine Brzezinski**[4], **Melissa D. Bauman**[3], **Allyson Alexander**[4], **Ann C. McKee**[2,5,6,7,8], **Thor D. Stein**[5,6,7,8], **Matthew Schall**[1], **Bob Jacobs**[1]

[1]Laboratory of Quantitative Neuromorphology, Neuroscience Program, Department of Psychology, Colorado College, Colorado Springs, Colorado

[2]Department of Neurology, Boston University School of Medicine, Boston, Massachusetts

[3]Department of Psychiatry and Behavioral Sciences, University of California, Sacramento, California

[4]Department of Neurosurgery, University of Colorado Anschutz Medical Campus, Aurora, Colorado

[5]Department of Pathology and Laboratory Medicine, Boston University School of Medicine, Boston, Massachusetts

[6]Boston University Alzheimer's Disease and CTE Center, Boston University School of Medicine, Boston, Massachusetts

[7]VA Boston Healthcare System, Boston, Massachusetts

[8]Department of Veterans Affairs Medical Center, Bedford, Massachusetts

Correspondence Allysa Warling and Bob Jacobs, Laboratory of Quantitative Neuromorphology, Neuroscience Program, Department of Psychology, Colorado College, 14 E. Cache La Poudre, Colorado Springs, CO 80903. allysa.warling@nih.gov (A. W.) and bjacobs@coloradocollege.edu (B. J.).

Abstract

Chronic traumatic encephalopathy (CTE) is a neurodegenerative disorder that is associated with repetitive head impacts. Neuropathologically, it is defined by the presence of perivascular hyperphosphorylated tau aggregates in cortical tissue (McKee et al., 2016, *Acta Neuropathologica*, 131, 75–86). Although many pathological and assumed clinical correlates of CTE have been well characterized, its effects on cortical dendritic arbors are still unknown. Here, we quantified dendrites and dendritic spines of supragranular pyramidal neurons in tissue from human frontal and occipital lobes, in 11 cases with ($M_{age} = 79 \pm 7$ years) and 5 cases without ($M_{age} = 76 \pm 11$ years) CTE. Tissue was stained with a modified rapid Golgi technique. Dendritic systems of 20 neurons per region in each brain ($N = 640$ neurons) were quantified using computer-assisted morphometry. One key finding was that CTE neurons exhibited increased variability and distributional changes across six of the eight dendritic system measures, presumably due to ongoing degeneration and compensatory reorganization of dendritic systems. However, despite heightened variation among CTE neurons, CTE cases exhibited lower mean values than Control cases in seven of the eight dendritic system measures. These dendritic alterations may represent a new pathological marker of CTE, and further examination of dendritic changes could contribute to both mechanistic and functional understandings of the disease.

Keywords

1 | INTRODUCTION

Chronic traumatic encephalopathy (CTE) is a neurodegenerative disorder typically associated with exposure to repetitive head impacts (RHIs) (Corsellis, Bruton, & Freeman-Browne, 1973; Martland, 1928; McKee et al., 2013; Omalu et al., 2005; Stern et al., 2011). RHIs, which include both concussive and subconcussive blows, affect dendritic and white matter integrity (Castejón & Arismendi, 2003; Coughlin et al., 2017; Mayinger et al., 2018). CTE, which may appear decades after RHI exposure, is characterized by the abnormal aggregation of hyperphosphorylated tau (a microtubule-associated protein; p-tau) in neurons and astrocytes (Bieniek et al., 2015; Ling et al., 2017; McKee et al., 2009; Mez et al., 2017), especially around small vessels in the depths of cortical sulci (McKee et al., 2016). It shares pathological protein aggregations and some clinical symptoms with Alzheimer's disease (Arena et al., 2020; Schmidt, Zhukareva, Newell, Lee, & Trojanowski, 2001; Stein et al., 2015; Stern et al., 2013; Woerman et al., 2016), which also impacts cortical dendritic systems (Hof & Morrison, 1990; Mavroudis et al., 2011; A. B. Scheibel & Tomiyasu, 1978). Although many neuroanatomical correlates of CTE are well characterized (e.g., p-tau pathology, gross gray matter loss, TDP-43 inclusions; Saing et al., 2012), the relationship between CTE and cortical dendrites remains unknown. Here, we provide a preliminary exploration of dendritic changes in CTE by quantifying the dendritic systems of supragranular (Layers II and III) pyramidal neurons in the frontal and occipital poles of human tissue.

Examination of pyramidal neuron dendrites may provide insight into neurodegenerative mechanisms in CTE. Current theories implicate prion-like spreading of p-tau following initial local hyperphosphorylation and misfolding, but the precise neurobiological pathways are unclear (Armstrong, McKee, Alvarez, & Cairns, 2017; Goedert, Clavaguera, & Tolnay, 2010). Although frontal and occipital lobes are both vulnerable in acute RHI (Bendlin et al., 2008; Ghajari, Hellyer, & Sharp, 2017; Lipton et al., 2013), the frontal lobe appears to be more affected in CTE (McKee et al., 2013; McKee, Daneshvar, Alvarez, & Stein, 2014). In CTE, the frontal lobe exhibits reduced macroscopic gray matter volume (McKee et al., 2013) and extensive p-tau aggregates, especially in supragranular cortical layers (Armstrong, McKee, Stein, Alvarez, & Cairns, 2019; Gavett, Stern, & McKee, 2011; McKee et al., 2016). The occipital lobe, in contrast, is spared of p-tau pathology (McKee et al., 2016). In healthy tissue, tau is enriched in pyramidal neuron axons. However, it migrates to dendrites under neurodegenerative conditions (Bancher et al., 1987; Ittner & Ittner, 2018), which impairs dendritic/spine function (Hoover et al., 2010; Merino-Serrais et al., 2013). Thus, examining dendritic arbors in regions with different vulnerabilities in CTE could provide further insight into p-tau-mediated disease processes.

Dendritic changes in CTE could also have functional implications. Supragranular pyramidal cells are key players in the networks that support cognitive processes (Gerfen, Paletzki, & Heintz, 2013; Harris & Shepherd, 2015; Meyer, 1987). Input to these neurons is mostly synthesized by their dendrites and spines, which exhibit considerable experience-dependent plasticity (Fu & Zuo, 2011; Gray, 1959). Thus, the physical properties of dendritic systems are intimately tied to their functions (Goriounova et al., 2018). Pyramidal neuron dendritic arbors in the frontal pole, a higher-order, integrative supramodal association region (Benson, 1993; Elston, 2000; Elston, Benavides-Piccione, Elston, Manger, & Defelipe, 2011; Miller & Cohen, 2001), are more extensive and have greater spine density than those in the occipital pole, a unimodal association region responsible for visual processing (Hegdé & Van Essen, 2000; Jacobs et al., 2001; Jacobs, Driscoll, & Schall, 1997; Willmore, Prenger, & Gallant, 2010). Dendritic degeneration has previously been linked to cognitive decline in Alzheimer's disease (Akram et al., 2008; DeKosky & Scheff, 1990; Mi et al., 2017; Terry et al., 1991), strengthening the case for quantifying dendritic systems in CTE tissue.

Although we consider the current investigation to be exploratory and partially descriptive in nature, previous research suggests several possible outcomes. Given that head injury and tauopathy are associated with both degenerative dendritic changes and compensatory dendritic arborization (Blennow, Hardy, & Zetterberg, 2012; Keyvani & Schallert, 2002; A. B. Scheibel & Tomiyasu, 1978), it is expected that neuronal measures in CTE cases will exhibit more dendritic variability and distributional changes compared to Control brains. Such complex degenerative and regenerative responses to damage pose analytical challenges in quantitative dendritic analyses that will need to be addressed. Despite potential variability in CTE tissue, the primary hypothesis is that dendritic systems will ultimately be more compromised in the CTE group than in the Control group. We also have several secondary predictions. First, as noted in prior research on normative tissue (Jacobs et al., 1997, 2001), the frontal lobe will exhibit more extensive dendritic arborization than the occipital lobe. Given its extensive p-tau burden (McKee et al., 2016), however, we expect frontal lobe CTE dendrites to be more compromised than occipital lobe CTE dendrites. Second, distal (fourth

order and higher) basilar dendritic segments, which tend to be more sensitive to epigenetic influences and the delayed effects of trauma (Carughi, Carpenter, & Diamond, 1989; Jacobs, Batal, et al., 1993; A. B. Scheibel et al., 1985), will be more compromised than proximal branches (first to third order). Third, due to specializations in integrative properties (Globus & Scheibel, 1967; Holthoff, Tsay, & Yuste, 2002; Larkum, Zhu, & Sakmann, 1999; Park et al., 2019), there may be differences in the amount of deterioration between apical and basilar dendrites in CTE brains.

2 | MATERIALS AND METHODS

2.1 | Subjects

For the CTE group, tissue from 11 male cases with a history of sportsrelated RHI (M_{age} = 79 ± 7 years; see Table 1) was obtained from the Veterans Affairs-Boston University-Concussion Legacy Foundation Brain Bank at the BU Alzheimer's Disease and CTE Center (Boston, MA). A CTE diagnosis was confirmed using established National Institute of Neurological Disease and Stroke/National Institute of Biomedical Imaging and Bioengineering neuropathological criteria (McKee et al., 2016). Each case was assigned a CTE Stage based on previously proposed guidelines (McKee et al., 2013): one case was Stage I (minimal, focal ptau pathology), five cases were Stage III (substantial p-tau pathology), and five cases were Stage IV (severe, widespread p-tau pathology). Additionally, neuropathologists, blinded to the participant's RHI exposure and clinical history, recorded semi-quantitative measures of p-tau immunoreactive neurofibrillary tangle (NFT) burden (by AT8 immunostaining) on a 0–3 scale (in increasing severity) for regions near those sampled for Golgi staining (i.e., dorsolateral prefrontal cortex and calcarine cortex) (Mez et al., 2020, see Table 1). For the Control group, tissue from five neurologically normal cases with no reported RHI exposure (M_{age} = 76 ± 11 years; four males, one female) was obtained from the Miami Brain Endowment Bank (Miami, FL) and the University of California-Davis Brain Bank (Davis, CA). Autolysis time (AT) averaged 31 ± 12 hr for the CTE group, and 18± 6 hr for the Control group. CTE brains were immersion fixed in 10% neutral buffered formalin for an average of 5 ± 3 months of fixation time (FT) prior to staining compared to 16 ± 8 months for Control brains. Relevant historical information for all cases was obtained from autopsy reports, medical records, and family interviews (McKee et al., 2013). The protocol was approved by the Colorado College Institutional Review Board (#011311-1).

2.2 | Tissue selection and preparation

Tissue blocks (1–2 cm in length) were removed from left or right frontal and occipital poles (as in Jacobs et al., 1997). In the prefrontal lobe, the tissue block was located approximately 1.5 cm lateral to the midline and 4 cm superior to the orbitomedial surface, a region generally corresponding to Brodmann's area (BA) 10 (Brodmann, 1909; Figure 1). In the occipital lobe, the tissue block was located approximately 1.5 cm superior to the inferior surface of the occipital lobe and 2 cm from the midline, a region generally corresponding to BA18. There was no reason to expect significant interhemispheric (Jacobs, Schall, & Scheibel, 1993) or between-sex (Jacobs et al., 1997, 2001) dendritic differences. The blocks were trimmed to 3–5 mm in anteroposterior thickness, processed using a modified rapid Golgi technique (M. E. Scheibel & Scheibel, 1978) and serially sectioned at 120 μm

with a vibratome (Leica VT1000S, Leica Microsystems, Wetzlar, Germany) such that the preparation was vertical to the pial surface and perpendicular to the long axis of the gyrus. Tissue blocks were coded to avoid experimenter bias.

2.3 | Neuron selection criteria and data collection

A total of 40 supragranular pyramidal neurons were traced in each brain (20 from each lobe). Selection criteria, detailed elsewhere (Jacobs et al., 1997, 2001; Jacobs, Schall, et al., 1993), required neurons to be well impregnated and relatively isolated, have a soma centrally located within the 120 μm section, and have a relatively complete dendritic arbor with an apical dendrite that was perpendicular to the pial surface.

Neurons were reconstructed along x-, y-, and z-coordinates under a planachromat ×60 (N.A. 1.4) oil objective, interfaced with an Olympus BH-1 microscope. The microscope was equipped with a Ludl XY motorized stage (Ludl Electronics, Hawthorne, NY), and a Heidenhain z-axis encoder (Schaumburg, IL). Data were collected using a Neurolucida camera system (v2018.2.2, MBF Bioscience, Williston, VT; RRID:SCR_001775), which projected images onto a 3,840 × 2,160 resolution Asus PA329Q 32-in. 4 K monitor using a MicroFire Digital CCD 2-Megapixel camera (Optronics, Goleta, CA) mounted on a trinocular head (Model 1-L0229, Olympus, Center Valley, PA).

The soma was traced at its widest point within the twodimensional plane to provide an estimate of cross-sectional area. Then, basilar and apical dendritic processes were traced, accounting for visible spines and dendritic diameter. Broken dendritic tips and ambiguous terminations were marked as incomplete. Thus, of the 28,708 terminal segments quantified, 12% were complete (CTE, BA10: 15%; CTE, BA18: 13%; Control, BA10: 12%; Control, BA18: 9%), leaving 88% (CTE, BA10: 85%; CTE, BA18: 87%; Control, BA10: 88%; Control, BA10: 91%) as incomplete. Although this number of incomplete segments was relatively high (see Jacobs et al., 2001), we were very conservative in our marking of complete endings. Moreover, the percentages were similar across both CTE and Control groups, and across cortical areas. Dendrites were not traced into adjacent tissue sections. Neurons with sectioned segments were not excluded, as this would have biased the sample towards smaller neurons (Uylings, Ruiz-Marcos, & Pelt, 1986). Additionally, because soma depth is positively correlated with soma size and dendritic branching (Jacobs et al., 2001; Matsubara, Chase, & Thejomayen, 1996), a running average of soma depth from the pial surface was maintained. Final averages (Control, BA10: 888 ± 256 μm; Control, BA18: 860 ± 201 μm; CTE, BA10: 870 ± 179 μm; CTE, BA18: 851 ± 187 μm) suggested relative consistency of neuronal depth across cortical areas and case cohorts. Although adjacent tissue sections were not available for Nissl stains, based on the laminar depths in a study that quantified dendritic systems in these same regions in an older cohort of healthy controls (n = 16, M_{age} = 71 ± 13 years; Jacobs et al., 1997), approximately 97% of neurons traced in CTE tissue were located in layer III, compared to 97.5% of neurons in Control tissue.

Neurons were traced by six investigators (A. W., R. U., H. S., C. D., M. E. G., N. B. S. S.). Intrarater reliability was assessed by having each investigator trace the same soma and dendritic segment 10 times. The average coefficients of variation for soma size (3.1%), total dendritic length (TDL, 1.4%), and dendritic spine number (DSN, 4.0%) indicated little

variation in the tracings. An additional split-plot design (a = .05) indicated no significant differences between the first five and last five tracings for any of the investigators. Interrater reliability was established by comparing tracings completed by each investigator to those completed by the primary investigator (B. J.). Average interclass correlations for soma size (1.00), TDL (0.99), and DSN (0.99) indicated no significant differences in these measures among investigators. All tracings were also reexamined under the microscope by the primary investigator to ensure accuracy.

2.4 | Quantitative dendritic and spine measures

Measures from reconstructed dendritic systems were quantified using a centrifugal nomenclature (Bok, 1959; Uylings et al., 1986): dendritic branches arising from the soma are first-order segments until they bifurcate into second-order segments, which branch into third-order segments, and so on. For basilar dendrites, the first three orders of segments were classified as proximal branches; fourthorder and above were classified as distal. Six previously established measures (Butti et al., 2015; Jacobs et al., 1997, 2011; Nguyen et al., 2020) were used to characterize each neuron's dendritic systems: dendritic volume (Vol, μm^3: the total volume of all dendrites), TDL (μm: the summed length of all dendritic segments), mean segment length (MSL, μm: the average length of each dendritic segment), dendritic segment count (DSC, the number of dendritic segments), DSN (the total number of spines on each neuron), and dendritic spine density (DSD, the average number of spines per μm of dendritic length). In addition, dendritic diameter (Dia, μm: the average thickness of individual dendritic processes) was measured. All descriptive measures are presented as mean ± *SEM* unless noted otherwise.

2.5 | Statistical analysis

To evaluate the stated hypotheses beyond the descriptive level, differences in dendritic measures—in terms of the mean, median, variance, skew, and kurtosis values—were evaluated between the CTE and Control groups. Although such hypotheses are typically evaluated using parametric tests for means (e.g., *t* tests or analysis of variances), there were three concerns about the appropriateness of such analytic approaches. First, past research (Jacobs et al., 2014, 2015, 2018; Johnson et al., 2016; Nguyen et al., 2020) indicated that some dendritic measures would not be normally distributed (with leptokurtoses being the most common issue), violating the normality assumptions of most such tests. Second, the data were repeated measurements (in the statistical sense) of the same neuronal branch, with each dendrite in turn nested within neuron, area, hemisphere, and brain. The repeated measures and nested nature of the data violate the assumption of independence in parametric tests and could introduce spurious correlations (Jacobs et al., 2014). Third, there was concern about the potential confounding effects of FT, AT, and soma depth. FT is seldom considered in quantitative Golgi studies (Buell, 1982; Butti et al., 2015), but AT is known to have a negative effect on dendritic systems (de Ruiter, 1983; Williams, Ferrante, & Caviness, 1978). Soma depth, although relatively controlled in the selection of neurons, could still affect dendritic measures. We thus needed a model that could address these specific confounds.

To this end, several preliminary analyses were performed. First, skew and kurtosis values were calculated. Because many of the attributes used to assess dendritic characteristics are transformations of common elements, only relationships between the relatively structurally unrelated attributes of DSN, Vol, TDL, soma size, and CTEStage (graded from 0 for Control, 15 for Stage I, 35 for Stage III, and 40 for Stage IV) were included. Correlational relationships were examined in three ways: (a) a factor analysis with one factor extracted using squared multiple correlation coefficients as communalities under the hypothesis that, if repeated measures or nesting caused association between the attributes, a single largest factor would emerge with an eigenvalue greater than two variables variance (i.e., greater than 2.0); (b) a Cronbach's alpha was calculated, where traditionally a value greater than .8 or .9 would indicate a set of items that reliably measure a common component, and a value less than a conservative .5 was taken as an indication of little induced correlation; and (c) a structural equation model or causal model (EQS Version 6.3) with an estimation method (arbitrary generalized least squares or AGLS) appropriate for attributes with significant skew and kurtosis was fit to the data to evaluate its structure. Model fit was evaluated using a model chi-square and the Yaun–Bentler AGLS F statistic, both with a null hypothesis that the model satisfactorily reproduced the original input data to the extent that conclusions could be made. Error paths for the regression equations were fixed at 1.0 unless the errors were correlated. A model that fits the data without a latent variable, and with no indication of a need to include a factor based on the regression paths, was considered indication of sufficient independence among the attributes to use t or F tests. Potential confounding effects were examined using the model. Confounds were placed between the independent neuronal measures and the outcome measure CTEStage. The presence of significant paths from the dendritic measures through the confounds to the target would be an indication that FT, AT, and/or soma depth had to be modeled. In this case, a multivariate adaptive regression splines (MARSplines, Statistica, release 13.3; StatSoft, Austin, TX; Friedman, 1991) analysis was used with the confounds in the model, making their contribution explicit and evaluable. MARSplines is a quantitative, nonparametric methodology (Hastie, Tibshirani, & Friedman, 2009) robust to violations of normality, nonhomogeneity of variability, and independence (Butti et al., 2015; Jacobs et al., 2014, 2015; Johnson et al., 2016; Nguyen et al., 2020). It was limited to a maximum of 30 basis functions, up to sixth-order interactions to accommodate the three confounds and the dendritic measures, a threshold of 0.0005, pruning was allowed, and penalty was set at 2. The null hypothesis was the same as in a comparable t or F test and was evaluated using a χ^2 from a correct and incorrect classification table. In the MARSplines analysis, predictor importance is the number of times each attribute is used in the resulting equations. The more times an attribute appears in the results, the more important it is in differentiating the variable under investigation.

Initially, disaggregated data were examined ($N = 53{,}782$ dendritic branches), with kurtoses ranging from near 0 to 212. Subsequent analyses were performed on aggregated-by-cell data ($N = 640$ neurons), which reduced kurtosis to a maximum of nearly six. Evaluation of the factor analytic results showed an eigenvalue of 2.30, indicating 46% common variance among the measures. A causal model without factors was successfully fit to the data ($\chi^2[9,640] = 12.19$, $p < .20$; $F[9,640] = 1.34$, $p < .21$), and failed to reject the null hypothesis that the model adequately reproduced the input data. In the model, there

were 51 significant regression and correlation paths between only 9 attributes, indicating considerable complexity in relationships among the predictors, confounds, and CTE group status, which could not have been ascertained with simpler or more traditional statistical approaches. Cronbach's alpha was .21, indicating a lack of an underlying reliable construct, although this analysis also included the three confounds, which might have reduced the value. The mixed results of a single factor accounting for 46% of the variance indicating some underlying commonality, a model fit with no factors, and <0.5 Cronbach's alpha necessitated the use of MARSplines for subsequent analyses.

3 | RESULTS

3.1 | Overview

Despite the typical interindividual variability that characterizes human tissue, results suggested potential differences between Control and CTE neurons. The Golgi preparations were of relatively high quality for nonperfused tissue (Figure 2), displaying few autolytic changes (Williams et al., 1978) and allowing the tracing of both apical and basilar dendrites. On the whole, dendritic variability was considerably greater in CTE brains than in Control brains. Additionally, descriptive findings indicated that mean dendritic and spine measures tended to be higher in BA10 than in BA18 in Control cases and that differences in neuronal measures between Control and CTE groups were greater for BA10 than BA18 (Figures 3 and 4). These trends held across both apical and basilar systems (Figure 5) and, consistent with these observations, quantitative tau pathology scores were higher in the prefrontal lobe (mean = 2 ± 1) than in the occipital lobe (mean = 0.36 ± 0.67) for every CTE case (Table 1). Distal basilar segments also seemed to be more vulnerable in CTE cases than proximal basilar segments (Figure 6). Although these descriptive trends are presented in detail below, they must be interpreted with caution and tempered by the statistical results that follow.

3.2 | Descriptive results for dendritic and spine measures

Examination of the five dendritic measures (Vol, TDL, DSC, MSL, and Dia) suggested between-group mean differences, with those differences being more pronounced in BA10 than in BA18. Compared to Control group neurons, dendritic Vol (Figure 4a) and Dia (Figure 4g) were lower in CTE group neurons in both BA10 (Vol by 26%; Dia by 30%) and BA18 (Vol by 12%; Dia by 28%). Although BA10 TDL (Figure 4b) and DSC (Figure 4d) measures were lower in the CTE group (TDL by 14%; DSC by 13%), these measures showed little (i.e., <5%) differences in BA18 between Control and CTE cases, suggesting that CTE-associated decreases in dendritic extent were more consistent in BA10 than in BA18. Between-group differences in MSL (Figure 4c) were negligible (i.e., <5% difference) for both regions.

These trends generally held when basilar and apical dendritic measures were considered separately. For example, both apical and basilar Vol (Figure 5a) and Dia (Figure 5g) measures were lower (i.e., > 5% lower) in CTE cases than in Control cases in both cortical areas. Mirroring the above results, both apical and basilar TDL (Figure 5b) and DSC (Figure 5d) exhibited relatively greater between-group differences in BA10 than in BA18, and the between-group differences for MSL were not notable (i.e., <5%) in either region for either

apical or basilar trees (Figure 5c). Across measures, there did not appear to be a consistent difference in vulnerability to CTE-associated decreases between apical and basilar arbors: Basilar Vol decreased relatively more in CTE tissue than did apical Vol in both BA10 and BA18, while apical TDL and DSC decreased more than basilar TDL and DSC in CTE tissue in BA10, and, in BA18, basilar TDL and DSC were actually higher in CTE tissue than in Control tissue.

In BA10, however, distal and proximal basilar dendrites appeared to be differentially affected in CTE cases. For dendritic Vol (Figure 6a), TDL (Figure 6b), and DSC (Figure 6d), CTE-associated decreases were 7–20% greater in distal than in proximal measures. BA10 Dia and MSL exhibited little difference between proximal and distal basilar measures (i.e., less than 5% difference in CTE-associated changes between proximal and distal branches), and findings in BA18 varied across measures. Thus, overall, the dendritic measures suggest a decrease in basilar and apical dendritic extent in frontal lobe neurons in CTE, and that distal basilar branches are most affected.

The two dendritic spine measures (DSN, DSD) also supported greater frontal lobe vulnerability in CTE. In BA10, DSN (Figure 4e) and DSD (Figure 4f) were lower in CTE than Control cases (DSN by 28%; DSD by 18%). In BA18, by contrast, these measures were higher (DSN by 16%; DSD by 13%) in CTE cases. Similar trends were observed for both measures when apical and basilar dendrites were considered separately (Figure 5e,f). Spine measures also implied increased vulnerability in distal basilar branches compared to proximal branches in BA10. Distal dendrites exhibited 32% lower DSN in the CTE group than in the Control group (Figure 6e), but, for proximal dendrites, DSN was only 11% lower. Distal DSD was 17% lower in CTE than in the Control group (Figure 6f), but was only 10% lower in proximal dendrites. Again, BA18 findings were not consistent between the two measures.

3.3 | Statistical analysis results

The primary hypothesis that dendritic systems would be more compromised in CTE compared to Controls was confirmed. Application of MARSplines identified a dendritic tree as Control or CTE with 96.2% accuracy. The null hypothesis of no difference between measures for CTE versus Control was rejected [$\chi^2(1,1,280) = 1,062.06$, $p < 0.0001$]. Measured based on number of occurrences in the MARSplines equations, and in order of importance, the predictors were FT (17), DSD (13), Dia (6), MSL (5), soma depth (4), soma size (4), TDL (2), AT (1), with Vol, DSC, and DSN having zero occurrences. The CTE group had many more extreme values (Table 2) even though the medians were homologous. Although the MARSplines results correctly indicated this difference, a simple t or F test would not have. Furthermore, the FT confound was the most entered component in the MARSplines equation, which indicated that an analysis without the confounds would have been inappropriate.

Hypothesis #2, that dendritic systems in the frontal lobe would be more compromised than those in the occipital lobe in the CTE group, was not confirmed. Review of MARSplines results indicated a dendritic tree as frontal or occipital with 74.2% accuracy. The null hypothesis of no difference between measures using frontal versus occipital region as the

dependent variable was rejected [$\chi^2(1,1,280) = 301.16$, $p < 0.000$]. Predictor importance was soma depth (7), Dia (6), soma size (6), DSD (5), DSN (4), MSL (3), Vol (2), TDL (2), DSC (2), FT (1), with CTE and AT not entering the equations. That CTE did not predict occipital versus frontal indicated that dendritic measures differed but not necessarily due to disease-related factors. A subsequent test using just the confounds and CTE to predict BA was only 54.7% accurate, which indicated that CTE as measured here may have had little differential impact on frontal versus occipital areas.

Hypothesis #3, that distal basilar dendritic segments would be more compromised in the CTE group than in the Control group, was not confirmed. Review of MARSplines results using distal versus proximal as the dependent variable identified dendrite origin with 93.9% accuracy. The null hypothesis of no difference between measures for proximal versus distal segments was rejected [$\chi^2(1,1,272) = 979.12$, $P < 0.0001$]. Predictor importance was Vol (11), Dia (8), MSL (7), FT (5), TDL (4), DSN (2), soma size (2), with DSC, DSD, soma depth, AT, and CTE not entering the equations. Although proximal versus distal was well predicted, CTE did not contribute. A subsequent test using just the confounds and CTE to predict proximal versus distal was only 50.3% accurate, which indicates that CTE had little differential effect on proximal versus distal dendritic systems.

Finally, Hypothesis #4 evaluated differences in apical versus basilar dendrites by using that attribute as the dependent measure to explore differences in response to CTE. Analysis of MARSplines output indicated a segment as apical or basilar with 77.5% accuracy. The null hypothesis of no difference between apical and basilar segments was rejected [$\chi^2(1,1,280) = 388.30$, $p < 0.0001$]. Predictor importance was Vol (6), DSC (4), DSD (4), soma size (3), FT (3), TDL (2), Dia (2), MSL (1), and soma depth (1), with DSN, AT, and CTE unrepresented. That is, CTE did not contribute to the differences between these dendritic arbors.

To more closely examine the confluent effects of degeneration and compensatory reorganization, distributional changes (as characterized by range, minimum, maximum, *SD*, skew, and kurtosis) were examined for the eight dendritic measures using Binomial *Z* tests under a null hypothesis of no difference between CTE and Control groups (Table 2). In general, most of the eight dendritic/spine measures had more extreme values for CTE than for Control (i.e., in 52 of 64 comparisons). In 12 of the 64 comparisons, Control results were more extreme than CTE results, with 5 of those associated with Dia and Vol measures. All values for MSL, DSC, DSD, and soma size were significantly more extreme in the CTE group [$Z = 2.04$, $p < 0.016$]. The distribution values for other dendritic measures were not significantly different between Control and CTE. This view of the data strongly suggests that CTE modified the distributions, despite having less of an impact on mean and median values.

4 | DISCUSSION

The present results documented CTE-associated changes in supragranular pyramidal cell dendritic complexity. As predicted in our primary hypothesis, there were overall decreases in the mean values of dendritic measures. However, these patterns were not consistent across all CTE neurons. CTE neurons exhibited increased variability and distributional changes in

dendritic/spine measures, presumably reflecting both disease-related damage and ongoing compensatory restructuring of dendritic systems. Descriptive analyses indicated a general CTE-related diminution of seven (Vol, TDL, DSC, DSN, DSD, Dia, and soma size) of the eight dependent measures examined, with decreases appearing to be greater in the frontal lobe than in the occipital lobe. A MARSplines analysis that controlled potential confounds and incorporated all of the dependent measures supported these observations and was able to correctly identify a dendritic tree as Control or CTE, despite the noted variability in CTE measures. Our secondary hypotheses attempted to refine the resolution of the study by examining dendritic differences between frontal versus occipital cortices, proximal versus distal basilar dendritic segments, and apical versus basilar dendritic extent. Although the descriptive measures were generally consistent with our predictions, the inferential statistical analyses failed to reject the null hypothesis of no difference in these secondary hypotheses.

4.1 | Methodological limitations

The methodological limitations typical of quantitative Golgi studies have been reviewed extensively (Braak & Braak, 1985; Jacobs et al., 1997, 2001; Jacobs, Schall, et al., 1993). Nevertheless, several issues specific to the present study remain. First, because tracing neurons within 120-μm-thick sections results in underestimations of dendritic measures, particularly for larger neurons, between-group differences (i.e., Control vs. CTE) in dendritic values were likely attenuated here (Jacobs et al., 1997, 2001). Second, the small number of cases, typical of quantitative Golgi studies (Anderson et al., 2009; Jacobs et al., 1997, 2001; Jacobs, Schall, et al., 1993; Jacobs & Scheibel, 1993), precluded specific examination of different CTE stages, although these stages were used in the causal model to understand the relationships among attributes. Finally, AT and FT were substantial confounds in the present study because AT was much longer in the CTE group, and FT was much longer in the Control group. Prolonged postmortem processes, which are often unavoidable in human studies, have deleterious effects on Golgi staining, particularly for spine measures (Butti et al., 2015; de Ruiter, 1983). This issue is addressed in more detail below.

4.2 | Overall dendritic changes in CTE

CTE tissue exhibited far greater between-neuron variability in dendritic measures (across Vol, Dia, TDL, MSL, DSC, and DSD) than Control tissue, suggesting CTE may be linked to a complex set of dendritic and spine changes (see ranges in Table 2). In this regard, CTE may not be a solely degenerative phenomenon, but may be accompanied by compensatory reorganization of cortical dendritic arbors. Such a process would account for both the upper and lower outlying values within the distributions of dendritic measures in CTE cases. It is also consistent with the dynamic responsiveness of dendritic arbors throughout the lifespan, whereby dendritic/spine growth and pruning accompany experience, sensory input, and physical environmental changes (Cheetham, Barnes, Albieri, Knott, & Finnerty, 2014; Diamond, Rosenzweig, Bennett, Lindner, & Lyon, 1972; Tavosanis, 2012; Trachtenberg et al., 2002). Additionally, dendritic outgrowth occurs following damage in acute head injury (Keyvani & Schallert, 2002) and in deafferentation following corpus callosotomy (Jacobs et al., 2003). Such growth appears to represent a compensatory process that accompanies integrative disruption. Finally, dendritic proliferation, in addition to atrophy, is present in

Alzheimer's disease (McKee, Kowall, & Kosik, 1989; A. B. Scheibel & Tomiyasu, 1978). Thus, compensatory dendritic reorganization in CTE is functionally plausible, compatible with known degenerative disease mechanisms, and consistent with the present findings.

Despite the observed variation, summed descriptive measures (i.e., Vol, TDL, DSN) and inferential analyses revealed an overall dendritic/spine decline in the CTE brains. Thus, the cumulative effect of dendritic changes was that of degeneration and loss. This putative loss fits with previously characterized neuropathological hallmarks of CTE. Dendritic arbors are compromised by p-tau aggregation (Hoover et al., 2010; Lee, Kim, Li, & Hall, 2012; Merino-Serrais et al., 2013; Regalado-Reyes, Benavides-Piccione, Fernaud-Espinosa, DeFelipe, & León-Espinosa, 2020), which is present in the superficial cortical layers in CTE (McKee et al., 2016), and are also affected by white matter disruption (Morquette et al., 2015), which has been described in CTE cases (Holleran et al., 2017). Dendritic changes could also underlie the macroscopic gray matter deficits previously noted in CTE brains (McKee et al., 2013; McKee et al., 2014), perhaps in concert with overt cellular loss. As with the compensatory processes described above, decreased dendritic extent is not unique to CTE—it is present in both normal aging (Jacobs et al., 1997) and in Alzheimer's disease (Uylings & de Brabander, 2002). However, the dendritic alterations observed in CTE brains relative to age-matched Controls suggest that, even if these mechanisms occur in the course of typical aging, they may be accelerated in CTE. Together, our findings support a model of dendritic change in CTE that is characterized by extensive loss alongside extreme intercellular variability. We posit that these dendritic proliferative changes represent an additional pathological characteristic of CTE.

4.3 | Examination of secondary hypotheses

Although our descriptive results generally supported our secondary hypotheses, inferential statistical results did not. The MARSplines analyses recorded no differences in CTE-associated changes between basilar and apical dendrites, nor between distal and proximal segments of basilar dendrites. In line with previous findings in healthy individuals (Jacobs et al., 1997, 2001), we found that frontal lobe neurons had more extensive dendritic arbors than occipital lobe neurons in the Control cohort. Compared to the occipital lobe, the frontal lobe carries a relatively greater pathological burden in CTE (in both in our present study and in past findings: Holleran et al., 2017; Mckee & Daneshvar, 2015; McKee et al., 2013, McKee et al., 2016). The greater presence of tau pathology in the prefrontal lobe than in the occipital lobe in our CTE subjects (Table 1; Alosco et al., 2020) is consistent with our descriptive findings, which suggested greater CTE-associated decreases in dendritic measures in the frontal lobe. Nevertheless, inferential analyses could not reliably differentiate between the two regions based on somatodendritic measures. This may be due to the extensive AT and FT for both cohorts in the present sample, which could have influenced analysis of between-group changes. To contextualize our present results and shed light on the potential confounds of FT and AT, we are fortunate to have data from a previous study (Jacobs et al., 1997), which examined basilar dendritic systems of supragranular pyramidal cells in BA10 and BA18 in neurologically normal subjects.

We used a subset of 12 age-matched individuals from this study ($M_{age} = 72 \pm 6$ years, range: 63–81; 8 males: $M_{age} = 71 \pm 5$ years; 4 females: $M_{age} = 74 \pm 6$ years), with much shorter AT (12 ± 7 hours) and FT (26 ± 13 days), as a Comparison cohort. A small methodological difference (e.g., use of a ×40, rather than ×60 objective) may have made cross-study comparisons of dendritic spine measures problematic (Anderson, Yamamoto, Kaplan, Hannan, & Jacobs, 2010), so here we only compare three dendritic measures: TDL, MSL, and DSC (Figure 7). The 1997 Comparison group exhibited much higher dendritic measures than either the Control or CTE cohort in both BA10 and BA18 (Figure 7). TDL for BA10 in the 1997 Comparison group was 38% higher than in the present Control group, and 47% higher than in the CTE group. Similarly, in BA18, TDL in 1997 Comparison group was 48% greater than in the present Control group, and 43% greater than in the CTE group. Comparable directional trends were seen for MSL and DSC measures. The greater dendritic extent observed in the 1997 Comparison group likely reflects the relatively shorter AT and FT in that sample (Butti et al., 2015) and implies that the observed differences between the present Control and CTE groups are probably underestimations. This may account for the lack of differences found in our secondary hypotheses and suggests that further study into regional and cellular-level dendritic changes in CTE is warranted.

4.4 | Pathological and functional implications

The present study supplements current theories about pathological and functional changes in CTE. In both CTE and Alzheimer's disease, hyperphosphorylated tau is the strongest candidate as a mediator of CTE-related dendritic alterations. Dendritic arbor changes could be driven by p-tau aggregation in dendritic processes (Hoover et al., 2010; Ittner & Ittner, 2018; Merino-Serrais et al., 2013) and/or be a postsynaptic consequence of axonal damage (Holleran et al., 2017; Morquette et al., 2015). Other potential contributing mechanisms include disruption in Ca^{2+} homeostasis and immunoexcitotoxicity, both of which are present in acute brain injury and neurodegenerative conditions (Blaylock & Maroon, 2011; Mattson, 2003; Ong, Tanaka, Dawe, Ittner, & Farooqui, 2013; Weber, 2004). We note that Dia was the dendritic measure most consistently diminished in our CTE cases (Table 2), and proper pyramidal cell Ca^{2+} regulation is closely tied to dendritic diameter (i.e., as it relates to surface-to-volume ratio; Holthoff et al., 2002; Regehr & Tank, 1994; Schiller, Helmchen, & Sakmann, 1995). We note further that soma size exhibited a seven times greater kurtosis value for CTE neurons compared to Control neurons, which suggests a number of considerably larger somata at the right-hand side of the distribution to form a positive tail. This may indicate additional neuronal pathology insofar as cytoplasmic swelling has been documented in some neurodegenerative diseases (Dickson et al., 2002; Dugger & Dickson, 2017). A design that directly correlates pathological burden with dendritic changes in CTE (as has been done with astrocytes; Hsu et al., 2018) could further distinguish the roles of differing pathological processes.

Finally, the observed dendritic changes in CTE may have functional consequences. The complexity of dendritic morphology reflects a neuron's integrative and processing capacities, with cortical regions involved in more complex functions supporting neurons with larger dendritic arbors (Anderson et al., 2009; Elston, 2000; Jacobs et al., 1997, 2001). Furthermore, dendritic extent has been linked to education attainment (Jacobs, Schall,

et al., 1993) and intellectual capacity (Goriounova et al., 2018) in healthy individuals, and dendritic/spine alterations are associated with the cognitive decline in Alzheimer's disease (Akram et al., 2008; DeKosky & Scheff, 1990; Mi et al., 2017). Although there are currently no validated *in vivo* diagnostic criteria for CTE, several cognitive symptoms have been reported in CTE cases (e.g., executive dysfunction, impulsivity, mood disturbances, dementia; Mez et al., 2017; Stern et al., 2013). Density of p-tau pathology, white matter abnormalities, and arteriosclerosis independently correlate with incidence of dementia in CTE cases (Alosco et al., 2019), but much about the neurobiological changes underlying cognitive symptoms remains unknown. Given the critical role of dendritic integrity in cortical processing (Gerfen et al., 2013; Harris & Shepherd, 2015; Meyer, 1987), dendritic decline may be a plausible intermediary between neuropathological processes and putative cognitive symptoms in CTE. Further work that considers dendritic changes in CTE alongside clinical symptoms is required to fully elucidate the connection.

5 | CONCLUSIONS

Here, we demonstrate that supragranular pyramidal neurons exhibit potential dendritic alterations in CTE, including increased variability and altered distributions in dendritic/spine measures, and overall decreases in dendritic extent. These alterations are consistent with pathological and functional changes in CTE. Further characterization of pyramidal cell dendrites in CTE may extend our mechanistic and functional understanding of this disease. We suggest that future quantitative neuromorphological studies prospectively control for factors such as AT and FT, and consider using sophisticated statistical methodology (Hesterberg, 2015) to accommodate potential confounds. In addition, future studies should look beyond measures of means and medians and examine measures such as variance and kurtosis to provide a greater distributional understanding dendritic changes.

ACKNOWLEDGMENTS

REFERENCES

Akram A, Christoffel D, Rocher AB, Bouras C, Kövari E, Perl DP, … Hof PR (2008). Stereologic estimates of total spinophilinimmunoreactive spine number in area 9 and the CA1 field: Relationship with the progression of Alzheimer's disease. Neurobiology of Aging, 29, 1296–1307. 10.1016/j.neurobiolaging.2007.03.007 [PubMed: 17420070]

Alosco ML, Cherry JD, Huber BR, Tripodis Y, Baucom Z, Kowall NW, … McKee AC (2020). Characterizing tau deposition in chronic traumatic encephalopathy (CTE): Utility of the McKee CTE staging scheme. Acta Neuropathologica. 10.1007/s00401-020-02197-9

Alosco ML, Stein TD, Tripodis Y, Chua AS, Kowall NW, Huber BR, … McKee AC (2019). Association of white matter rarefaction, arteriolosclerosis, and tau with dementia in chronic traumatic encephalopathy. Journal of the American Medical Association Neurology, 76, 1298–1308. 10.1001/jamaneurol.2019.2244 [PubMed: 31380975]

Anderson K, Bones B, Robinson B, Hass C, Lee H, Ford K, … Jacobs B. (2009). The morphology of supragranular pyramidal neurons in the human insular cortex: A quantitative Golgi study. Cerebral Cortex, 19, 2131–2144. 10.1093/cercor/bhn234 [PubMed: 19126800]

Anderson K, Yamamoto E, Kaplan J, Hannan M, & Jacobs B. (2010). Neurolucida lucivid versus neurolucida camera: A quantitative and qualitative comparison of three-dimensional neuronal reconstructions. Journal of Neuroscience Methods, 186, 209–214. 10.1016/j.jneumeth.2009.11.024 [PubMed: 19963008]

Arena JD, Smith DH, Lee EB, Gibbons GS, Irwin DJ, Robinson JL, … Johnson VE (2020). Tau immunophenotypes in chronic traumatic encephalopathy recapitulate those of ageing and Alzheimer's disease. Brain, 143, 1572–1587. 10.1093/brain/awaa071 [PubMed: 32390044]

Armstrong RA, McKee AC, Alvarez VE, & Cairns NJ (2017). Clustering of tau-immunoreactive pathology in chronic traumatic encephalopathy. Journal of Neural Transmission, 124, 185–192. 10.1007/s00702-016-1635-1 [PubMed: 27770214]

Armstrong RA, McKee AC, Stein TD, Alvarez VE, & Cairns NJ (2019). Cortical degeneration in chronic traumatic encephalopathy and Alzheimer's disease neuropathologic change. Neurological Sciences, 40, 529–533. 10.1007/s10072-018-3686-6 [PubMed: 30564964]

Bancher C, Lassmann H, Budka H, Grundke-Iqbal I, Iqbal K, Wiche G, … Wisniewski HM (1987). Neurofibrillary tangles in Alzheimer's disease and progressive supranuclear palsy: Antigenic similarities and differences. Microtubule-associated protein tau antigenicity is prominent in all types of tangles. Acta Neuropathologica, 74, 39–46. 10.1007/BF00688336 [PubMed: 2444063]

Bendlin BB, Ries ML, Lazar M, Alexander AL, Dempsey RJ, Rowley HA, … Johnson SC (2008). Longitudinal changes in patients with traumatic brain injury assessed with diffusion-tensor and volumetric imaging. NeuroImage, 42, 503–514. 10.1016/j.neuroimage.2008.04.254 [PubMed: 18556217]

Benson DF (1993). Prefrontal abilities. Behavioural Neurology, 6, 75–81. [PubMed: 24487070]

Bieniek KF, Ross OA, Cormier KA, Walton RL, Soto-Ortolaza A, Johnston AE, … Dickson DW (2015). Chronic traumatic encephalopathy pathology in a neurodegenerative disorders brain bank. Acta Neuropathologica, 130, 887–889. 10.1007/s00401-015-1502-4

Blaylock RL, & Maroon J. (2011). Immunoexcitotoxicity as a central mechanism in chronic traumatic encephalopathy—A unifying hypothesis. Surgical Neurology International, 2, 107. 10.4103/2152-7806.83391 [PubMed: 21886880]

Blennow K, Hardy J, & Zetterberg H. (2012). The neuropathology and neurobiology of traumatic brain injury. Neuron, 76, 886–899. 10.1016/j.neuron.2012.11.021 [PubMed: 23217738]

Bok ST (1959). Histonomy of the cerebral cortex. Amsterdam, The Netherlands: Elsevier.

Braak H, & Braak E. (1985). Golgi preparations as a tool in neuropathology with particular reference to investigations of the human telencephalic cortex. Progress in Neurobiology, 25, 93–139. 10.1016/0301-0082(85)90001-2 [PubMed: 2418465]

Brodmann K. (1909). Vergleichende Lokalisationlehre der Grosshirinde in ihren Prinzipien dargestellt auf Grund des Zellenbaues. [Comparative localization in the cerebral cortex: The principles of comparative localization in the cerebral cortex based on cytoarchitecture]. Leipzig: J. A. Barth.

Buell SJ (1982). Golgi-Cox and rapid Golgi methods as applied to autopsied human brain tissue: Widely disparate results. Journal of Neuropathology and Experimental Neurology, 41, 500–507. 10.1097/00005072-198209000-00003 [PubMed: 6180137]

Butti C, Janeway CM, Townshend C, Wicinski BA, Reidenberg JS, Ridgway SH, … Jacobs B. (2015). The neocortex of cetartiodactyls: I. A comparative Golgi analysis of neuronal morphology in the bottlenose dolphin (Tursiops truncatus), the minke whale (Balaenoptera acutorostrata), and

the humpback whale (Megaptera novaeangliae). Brain Structure and Function, 220, 3339–3368. 10.1007/s00429-014-0860-3 [PubMed: 25100560]

Carughi A, Carpenter KJ, & Diamond MC (1989). Effect of environmental enrichment during nutritional rehabilitation on body growth, blood parameters and cerebral cortical development of rats. The Journal of Nutrition, 119, 2005–2016. 10.1093/jn/119.12.2005 [PubMed: 2621493]

Castejón OJ, & Arismendi GJ (2003). Morphological changes of dendrites in the human edematous cerebral cortex. A transmission electron microscopic study. Journal of Submicroscopic Cytology and Pathology, 35, 395–413. [PubMed: 15137681]

Cheetham CEJ, Barnes SJ, Albieri G, Knott GW, & Finnerty GT (2014). Pansynaptic enlargement at adult cortical connections strengthened by experience. Cerebral Cortex, 24, 521–531. 10.10903/cer-cor/bhs334 [PubMed: 23118196]

Corsellis JA, Bruton CJ, & Freeman-Browne D. (1973). The aftermath of boxing. Psychological Medicine, 3, 270–303. 10.1017/S0033291700049588 [PubMed: 4729191]

Coughlin JM, Wang Y, Minn I, Bienko N, Ambinder EB, Xu X, … Pomper MG (2017). Imaging of glial cell activation and white matter integrity in brains of active and recently retired National Football League players. JAMA Neurology, 74, 67–74. 10.1001/jamaneurol.2016.3764 [PubMed: 27893897]

de Ruiter JP (1983). The influence of post-mortem fixation delay on the reliability of the Golgi silver impregnation. Brain Research, 266, 143–147. 10.1016/0006-8993(83)91317-3 [PubMed: 6189557]

DeKosky ST, & Scheff SW (1990). Synapse loss in frontal cortex biopsies in Alzheimer's disease: Correlation with cognitive severity. Annals of Neurology, 27, 457–464. 10.1002/ana.410270502 [PubMed: 2360787]

Diamond MC, Rosenzweig MR, Bennett EL, Lindner B, & Lyon L. (1972). Effects of environmental enrichment and impoverishment on rat cerebral cortex. Journal of Neurobiology, 3, 47–64. 10.1002/neu.480080105 [PubMed: 5028293]

Dickson DW, Bergeron C, Chin SS, Duyckaerts C, Horouplan D, Ikeda K, … Litvan I. (2002). Office of rare diseases neuropathological criteria for corticobasal degeneration. Journal of Neuropathology and Experimental Neurology, 61, 935–946. 10.1093/jnen/61.11.935 [PubMed: 12430710]

Dugger BN, & Dickson DW (2017). Pathology of neurodegenerative diseases. Cold Spring Harbor Perspectives in Biology, 9, a028035. 10.1101/cshperspect.a028035

Elston GN (2000). Pyramidal cells of the frontal lobe: All the more spinous to think with. The Journal of Neuroscience, 20(18), RC95. 10.1523/JNEUROSCI.20-18-j0002.2000

Elston GN, Benavides-Piccione R, Elston A, Manger PR, & Defelipe J. (2011). Pyramidal cells in prefrontal cortex of primates: Marked differences in neuronal structure among species. Frontiers in Neuroanatomy, 5, 2. 10.3389/fnana.2011.00002 [PubMed: 21347276]

Friedman JH (1991). Multivariate adaptive regression splines. The Annals of Statistics, 19, 1–67. 10.1214/aos/1176347963

Fu M, & Zuo Y. (2011). Experience-dependent structural plasticity in the cortex. Trends in Neurosciences, 34, 177–187. 10.1016/j.tins.2011.02.001 [PubMed: 21397343]

Gavett BE, Stern RA, & McKee AC (2011). Chronic traumatic encephalopathy: A potential late effect of sport-related concussive and subconcussive head trauma. Clinics in Sports Medicine, 30, 179–188. 10.1016/j.csm.2010.09.007 [PubMed: 21074091]

Gerfen CR, Paletzki R, & Heintz N. (2013). GENSAT BAC Crerecombinase driver lines to study the functional organization of cerebral cortical and basal ganglia circuits. Neuron, 80, 1368–1383. 10.1016/j.neuron.2013.10.016 [PubMed: 24360541]

Ghajari M, Hellyer PJ, & Sharp DJ (2017). Computational modelling of traumatic brain injury predicts the location of chronic traumatic encephalopathy pathology. Brain, 140, 333–343. 10.1093/brain/aww317 [PubMed: 28043957]

Globus A, & Scheibel AB (1967). Synaptic loci on visual cortical neurons of the rabbit: The specific afferent radiation. Experimental Neurology, 18, 116–131. 10.1016/0014-4886(67)90093-3 [PubMed: 4164552]

Goedert M, Clavaguera F, & Tolnay M. (2010). The propagation of prion-like protein inclusions in neurodegenerative diseases. Trends in Neurosciences, 33, 317–325. 10.1016/j.tins.2010.04.003 [PubMed: 20493564]

Goriounova NA, Heyer DB, Wilbers R, Verhoog MB, Giugliano M, Verbist C, … Mansvelder HD (2018). Large and fast human pyramidal neurons associate with intelligence. eLife, 7. 10.7554/eLife.41714

Gray EG (1959). Electron microscopy of synaptic contacts on dendrite spines of the cerebral cortex. Nature, 183, 1592–1593. 10.1038/1831592a0 [PubMed: 13666826]

Harris KD, & Shepherd GMG (2015). The neocortical circuit: Themes and variations. Nature Neuroscience, 18, 170–181. 10.1038/nn.3917 [PubMed: 25622573]

Hastie T, Tibshirani R, & Friedman J. (2009). The elements of statistical learning (2nd ed.). New York, NY: Springer.

Hegdé J, & Van Essen DC (2000). Selectivity for complex shapes in primate visual area V2. Journal of Neuroscience, 20, RC61. 10.1523/JNEUROSCI.20-05-j0001.2000

Hesterberg TC (2015). What teachers should know about the bootstrap: Resampling in the undergraduate statistics curriculum. The American Statistician, 69, 371–386. 10.1080/00031305/2015.1089789 [PubMed: 27019512]

Hof PR, & Morrison JH (1990). Quantitative analysis of a vulnerable subset of pyramidal neurons in Alzheimer's disease: II. Primary and secondary visual cortex. Journal of Comparative Neurology, 301, 55–64. 10.1002/cne.903010106

Holleran L, Kim JH, Gangolli M, Stein T, Alvarez V, McKee A, & Brody DL (2017). Axonal disruption in white matter underlying cortical sulcus tau pathology in chronic traumatic encephalopathy. Acta Neuropathologica, 133, 367–380. 10.1007/s00401-017-1686-x [PubMed: 28214960]

Holthoff K, Tsay D, & Yuste R. (2002). Calcium dynamics of spines depend on their dendritic location. Neuron, 33, 425–437. 10.1016/S0896-6273(02)00576-7 [PubMed: 11832229]

Hoover BR, Reed MN, Su J, Penrod RD, Kotilinek LA, Grant MK, … Liao D. (2010). Tau mislocalization to dendritic spines mediates synaptic dysfunction independently of neurodegeneration. Neuron, 68, 1067–1081. 10.1016/j.neuron.2010.11.030 [PubMed: 21172610]

Hsu ET, Gangolli M, Su S, Holleran L, Stein TD, Alvarez VE, … Brody DL (2018). Astrocytic degeneration in chronic traumatic encephalopathy. Acta Neuropathologica, 136, 955–972. [PubMed: 30194648]

Ittner A, & Ittner LM (2018). Dendritic Tau in Alzheimer's disease. Neuron, 99, 13–27. 10.1016/j.neuron.2018.06.003 [PubMed: 30001506]

Jacobs B, Batal HA, Lynch B, Ojemann G, Ojemann LM, & Scheibel AB (1993). Quantitative dendritic and spine analyses of speech cortices: A case study. Brain and Language, 44, 239–253. [PubMed: 8513402]

Jacobs B, Creswell J, Britt JP, Ford KL, Bogen JE, & Zaidel E. (2003). Quantitative analysis of cortical pyramidal neurons after corpus callosotomy. Annals of Neurology, 54, 126–130. 10.1002/ana.10620 [PubMed: 12838530]

Jacobs B, Driscoll L, & Schall M. (1997). Life-span dendritic and spine changes in areas 10 and 18 of the human cortex: A quantitative Golgi study. Journal of Comparative Neurology, 386, 661–680. 10.1002/(SICI)1096-9861(19971006)386:4<661::AID-CNE11>3.0.CO;2-N

Jacobs B, Garcia ME, Shea-Shumsky NB, Tennison ME, Schall M, Saviano MS, … Manger PR (2018). Comparative morphology of gigantopyramidal neurons in primary motor cortex across mammals. Journal of Comparative Neurology, 526, 496–536. 10.1002/cne.24349

Jacobs B, Harland T, Kennedy D, Schall M, Wicinski B, Butti C, … Manger PR (2015). The neocortex of cetartiodactyls. II. Neuronal morphology of the visual and motor cortices in the giraffe (Giraffa camelopardalis). Brain Structure and Function, 220, 2851–2872. 10.1007/s00429-014-0830-9 [PubMed: 25048683]

Jacobs B, Johnson NL, Wahl D, Schall M, Maseko BC, Lewandowski A, … Manger PR (2014). Comparative neuronal morphology of the cerebellar cortex in afrotherians, carnivores, cetartiodactyls, and primates. Frontiers in Neuroanatomy, 8, 24. 10.3389/fnana.2014.00024 [PubMed: 24795574]

Jacobs B, Lubs J, Hannan M, Anderson K, Butti C, Sherwood CS, … Manger PR (2011). Neuronal morphology in the African elephant (Loxodonta africana) neocortex. Brain Structure and Function, 215, 273–298. 10.1007/s00429-010-0288-3 [PubMed: 21079992]

Jacobs B, Schall M, Prather M, Kapler E, Driscoll L, Baca S, … Treml M. (2001). Regional dendritic and spine variation in human cerebral cortex: A quantitative Golgi study. Cerebral Cortex, 11, 558–571. 10.1093/cercor/11.6.558 [PubMed: 11375917]

Jacobs B, Schall M, & Scheibel AB (1993). A quantitative dendritic analysis of Wernicke's area in humans. II. Gender, hemispheric, and environmental factors. Journal of Comparative Neurology, 327, 97–111. 10.1002/cne.903270108

Jacobs B, & Scheibel AB (1993). A quantitative dendritic analysis of Wernicke's area in humans. I. Lifespan changes. Journal of Comparative Neurology, 327, 83–96. 10.1002/cne.903270107

Johnson CB, Schall M, Tennison ME, Garcia ME, Shea-Shumsky NB, Raghanti M, … Jacobs B. (2016). Neocortical neuronal morphology in the Siberian Tiger (Panthera tigris altaica) and the clouded leopard (Neofelis nebulosa). Journal of Comparative Neurology, 524, 3641–3665. 10.1002/cne.24022

Keyvani K, & Schallert T. (2002). Plasticity-associated molecular and structural events in the injured brain. Journal of Neuropathology and Experimental Neurology, 61, 831–840. 10.1093/jnen/61.10.831 [PubMed: 12387449]

Larkum ME, Zhu JJ, & Sakmann B. (1999). A new cellular mechanism for coupling inputs arriving at different cortical layers. Nature, 398, 338–341. 10.1038/18686 [PubMed: 10192334]

Lee S, Kim W, Li Z, & Hall GF (2012). Accumulation of vesicleassociated human tau in distal dendrites drives degeneration and tau secretion in an situ cellular tauopathy model. International Journal of Alzheimer's Disease, 2012, 1–16. 10.1155/2012/172837

Ling H, Morris HR, Neal JW, Lees AJ, Hardy J, Holton JL, … Williams DDR (2017). Mixed pathologies including chronic traumatic encephalopathy account for dementia in retired association football (soccer) players. Acta Neuropathologica, 133, 337–352. 10.1007/s00401-017-1680-3 [PubMed: 28205009]

Lipton ML, Kim N, Zimmerman ME, Kim M, Stewart WF, Branch CA, & Lipton RB (2013). Soccer heading is associated with white matter microstructural and cognitive abnormalities. Radiology, 268, 850–857. 10.1148/radiol.13130545 [PubMed: 23757503]

Martland HS (1928). Punch drunk. Journal of the American Medical Association, 91, 1103. 10.1001/jama.1928.02700150029009

Matsubara JA, Chase R, & Thejomayen M. (1996). Comparative morphology of three types of projection-identified pyramidal neurons in the superficial layers of cat visual cortex. Journal of Comparative Neurology, 366, 93–108. 10.1002/(SICI)1096-9861(19960226)366:1<93::AID-CNE7>3.0.CO;2-F

Mattson MP (2003). Excitotoxic and excitoprotective mechanisms: Abundant targets for the prevention and treatment of neurodegenerative disorders. Neuromolecular Medicine, 3, 65–94. 10.1385/NMM:3:2:65 [PubMed: 12728191]

Mavroudis IA, Fotiou DF, Manani MG, Njaou SN, Frangou D, Costa VG, & Baloyannis SJ (2011). Dendritic pathology and spinal loss in the visual cortex in Alzheimer's disease: A Golgi study in pathology. International Journal of Neuroscience, 121, 347–354. 10.3109/00207454.2011.553753

Mayinger MC, Merchant-Borna K, Hufschmidt J, Muehlmann M, Weir IR, Rauchmann B-S, … Bazarian JJ (2018). White matter alterations in college football players: A longitudinal diffusion tensor imaging study. Brain Imaging and Behavior, 12, 44–53. 10.1007/s11682-017-9672-4 [PubMed: 28092023]

McKee AC, Cairns NJ, Dickson DW, Folkerth RD, Dirk Keene C, Litvan I, … Gordon WA (2016). The first NINDS/NIBIB consensus meeting to define neuropathological criteria for the diagnosis of chronic traumatic encephalopathy. Acta Neuropathologica, 131, 75–86. 10.1007/s00401-015-1515-z [PubMed: 26667418]

McKee AC, Cantu RC, Nowinski CJ, Hedley-Whyte ET, Gavett BE, Budson AE, … Stern RA (2009). Chronic traumatic encephalopathy in athletes: Progressive tauopathy after repetitive head injury. Journal of Neuropathology and Experimental Neurology, 68, 709–735. 10.1097/NEN.0b013e3181a9d503 [PubMed: 19535999]

McKee AC, & Daneshvar DH (2015). The neuropathology of traumatic brain injury. Handbook of Clinical Neurology, 127, 45–66. 10.1016/B978-0-444-52892-6.00004-0 [PubMed: 25702209]

McKee AC, Daneshvar DH, Alvarez VE, & Stein TD (2014). The neuropathology of sport. Acta Neuropathologica, 127, 29–51. 10.1007/s00401-013-1230-6 [PubMed: 24366527]

McKee AC, Kowall NW, & Kosik KS (1989). Microtubular reorganization and dendritic growth response in Alzheimer's disease. Annals of Neurology, 26, 652–659. 10.1002/ana.410260511 [PubMed: 2817839]

McKee AC, Stern RA, Nowinski CJ, Stein TD, Alvarez VE, Daneshvar DH, … Cantu RC (2013). The spectrum of disease in chronic traumatic encephalopathy. Brain, 136, 43–64. 10.1093/brain/aws307 [PubMed: 23208308]

Merino-Serrais P, Benavides-Piccione R, Blazquez-Llorca L, Kastanauskaite A, Rábano A, Avila J, & DeFelipe J. (2013). The influence of phospho-tau on dendritic spines of cortical pyramidal neurons in patients with Alzheimer's disease. Brain, 136, 1913–1928. 10.1093/brain/awt088 [PubMed: 23715095]

Meyer G. (1987). Forms and spatial arrangement of neurons in the primary motor cortex of man. Journal of Comparative Neurology, 262, 402–428. 10.1002/cne.902620306

Mez J, Daneshvar DH, Abdolmohammadi B, Chua AS, Alosco ML, Kiernan PT, … McKee AC (2020). Duration of American football play and chronic traumatic encephalopathy. Annals of Neurology, 87, 116–131. 10.1002/ana.25611 [PubMed: 31589352]

Mez J, Daneshvar DH, Kiernan PT, Abdolmohammadi B, Alvarez VE, Huber BR, … McKee AC (2017). Clinicopathological evaluation of chronic traumatic encephalopathy in players of American football. Journal of the American Medical Association, 318, 360–370. 10.1001/jama.2017.8334 [PubMed: 28742910]

Mi Z, Abrahamson EE, Ryu AY, Fish KN, Sweet RA, Mufson EJ, & Ikonomovic MD (2017). Loss of precuneus dendritic spines immunopositive for spinophilin is related to cognitive impairment in early Alzheimer's disease. Neurobiology of Aging, 55, 159–166. 10.1016/j.neurobiolaging.2017.01.022 [PubMed: 28259365]

Miller EK, & Cohen JD (2001). An integrative theory of prefrontal cortex function. Annual Review of Neuroscience, 24, 167–202. 10.1146/annurev.neuro.24.1.167

Morquette B, Morquette P, Agostinone J, Feinstein E, McKinney RA, Kolta A, & Di Polo A. (2015). REDD2-mediated inhibition of mTOR promotes dendrite retraction induced by axonal injury. Cell Death and Differentiation, 22, 612–625. 10.1038/cdd.2014.149 [PubMed: 25257176]

Nguyen VT, Uchida R, Warling A, Sloan LJ, Saviano MS, Wicinski B, … Jacobs B. (2020). Comparative neocortical neuromorphology in felids: African lion, African leopard, and cheetah. Journal of Comparative Neurology, 528, 1392–1422. 10.1002/cne24823

Omalu BI, DeKosky ST, Minster RL, Kamboh MI, Hamilton RL, & Wecht CH (2005). Chronic traumatic encephalopathy in a National Football League player. Neurosurgery, 57, 128–134. 10.1227/01.NEU.000163407.92769.ED

Ong W-Y, Tanaka K, Dawe GS, Ittner LM, & Farooqui AA (2013). Slow excitotoxicity in Alzheimer's disease. Journal of Alzheimer's Disease, 35, 643–668. 10.3233/jad-121990

Park J, Papoutsi A, Ash RT, Marin MA, Poirazi P, & Smirnakis SM (2019). Contribution of apical and basal dendrites to orientation encoding in mouse V1 L2/3 pyramidal neurons. Nature Communications, 10, 5372. 10.1038/241467-019-13029-0

Regalado-Reyes M, Benavides-Piccione R, Fernaud-Espinosa I, DeFelipe J, & León-Espinosa G. (2020). Effect of phosphorylated tau on cortical pyramidal neuron morphology during hibernation. Cerebral Cortex Communications, tgaa018. 10.1093/texcom/tgaa018

Regehr WG, & Tank DW (1994). Dendritic calcium dynamics. Current Opinion in Neurobiology, 4, 373–382. 10.1016/0959-4388(94)90099-X [PubMed: 7919932]

Saing T, Dick M, Nelson PT, Kim RC, Cribbs DH, & Head E. (2012). Frontal cortex neuropathology in dementia pugilistica. Journal of Neurotrauma, 29, 1054–1070. 10.1089/neu.2011.1957 [PubMed: 22017610]

Scheibel AB, Paul LA, Fried I, Forsythe AB, Tomiyasu U, Wechsler A, … Slotnick J. (1985). Dendritic organization of the anterior speech area. Experimental Neurology, 87, 109–117. 10.1016/0014-4886(85)90137-2 [PubMed: 3967694]

Scheibel AB, & Tomiyasu U. (1978). Dendritic sprouting in Alzheimer's presenile dementia. Experimental Neurology, 60, 1–8. 10.1016/0014-4886(78)90164-4 [PubMed: 350599]

Scheibel ME, & Scheibel AB (1978). The methods of Golgi. In Robertson RT (Ed.), Neuroanatomical research techniques (pp. 89–114). New York, NY: Academic Press.

Schiller J, Helmchen F, & Sakmann B. (1995). Spatial profile of dendritic calcium transients evoked by action potentials in rat neocortical pyramidal neurons. Journal of Physiology, 487, 583–600. 10.1113/jphysiol.1995.sp020902

Schmidt M, Zhukareva V, Newell K, Lee V, & Trojanowski J. (2001). Tau isoform profile and phosphorylation state in dementia pugilistica recapitulate Alzheimer's disease. Acta Neuropathologica, 101, 518–524. 10.1007/s004010000330 [PubMed: 11484824]

Stein TD, Montenigro PH, Alvarez VE, Xia W, Crary JF, Tripodis Y, … McKee AC (2015). Beta-amyloid deposition in chronic traumatic encephalopathy. Acta Neuropathologica, 130, 21–34. 10.1007/s00401-015-1435 [PubMed: 25943889]

Stern RA, Daneshvar DH, Baugh CM, Seichepine DR, Montenigro PH, Riley DO, … McKee AC (2013). Clinical presentation of chronic traumatic encephalopathy. Neurology, 81, 1122–1129. 10.1212/WNL.0b013e3182a55f7f [PubMed: 23966253]

Stern RA, Riley DO, Daneshvar DH, Nowinski CJ, Cantu RC, & McKee AC (2011). Long-term consequences of repetitive brain trauma: Chronic traumatic encephalopathy. PM&R, 3, S460–S467. 10.1016/j.pmrj.2011.08.008 [PubMed: 22035690]

Tavosanis G. (2012). Dendritic structural plasticity. Developmental Neurobiology, 72, 73–86. 10.1002/dneu.20951 [PubMed: 21761575]

Terry RD, Masliah E, Salmon DP, Butters N, DeTeresa R, Hill R, … Katzman R. (1991). Physical basis of cognitive alterations in Alzheimer's disease: Synapse loss is the major correlate of cognitive impairment. Annals of Neurology, 30, 572–580. 10.1002/ana.410300410 [PubMed: 1789684]

Trachtenberg JT, Chen BE, Knott GW, Feng G, Sanes JR, Welker E, & Svoboda K. (2002). Long-term in vivo imaging of experience-dependent synaptic plasticity in adult cortex. Nature, 420, 788–794. 10.1038/nature01273 [PubMed: 12490942]

Uylings HBM, Ruiz-Marcos A, & Pelt JV (1986). The metric analysis of three-dimensional dendritic tree patterns: A methodological review. Journal of Neuroscience Methods, 18, 127–151. 10.1016/0165-0270(86)90116-0 [PubMed: 3540466]

Uylings HBM, & de Brabander JM (2002). Neuronal changes in normal human aging and Alzheimer's disease. Brain and Cognition, 49, 268–276. 10.1006/brcg.2001.1500 [PubMed: 12139954]

Weber J. (2004). Calcium homeostasis following traumatic neuronal injury. Current Neurovascular Research, 1, 151–171. 10.2174/1567202043480134 [PubMed: 16185191]

Williams RS, Ferrante RJ, & Caviness VS Jr. (1978). The Golgi rapid method in clinical neuropathology: The morphologic consequences of suboptimal fixation. Journal of Neuropathology and Experimental Neurology, 37, 13–33. 10.1097/00005072-197801000-00002 [PubMed: 73572]

Willmore BDB, Prenger RJ, & Gallant JL (2010). Neural representation of natural images in visual area V2. Journal of Neuroscience, 30, 2102–2114. 10.1523/JNEUROSCI.4099-09.2010 [PubMed: 20147538]

Woerman AL, Aoyagi A, Patel S, Kazmi SA, Lobach I, Grinberg LT, … Prusiner SB (2016). Tau prions from Alzheimer's disease and chronic traumatic encephalopathy patients propagate in cultured cells. Proceedings of the National Academy of Sciences, 113, E8187–E8196. 10.1073/pnas.1616344113
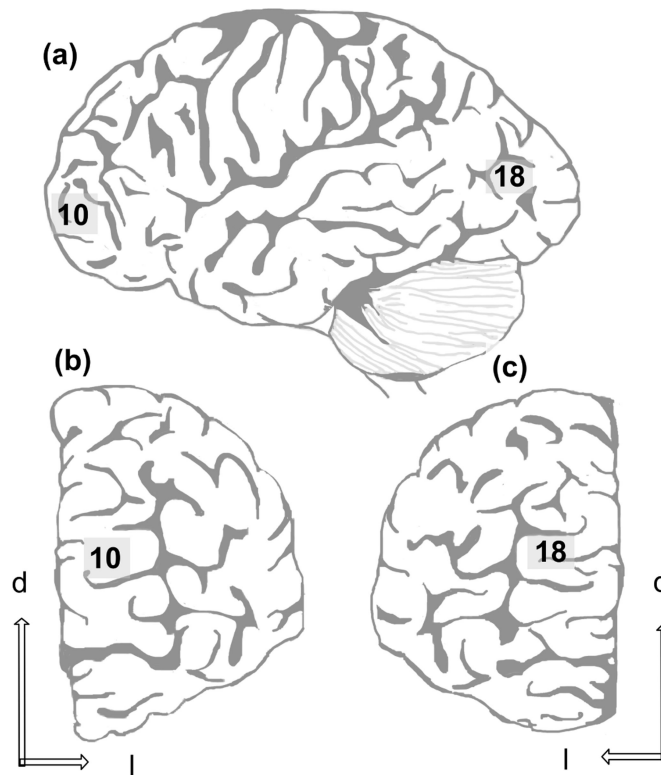
FIGURE 1.
Schematic of (a) lateral view of the left hemisphere, (b) the frontal pole, and (c) the occipital pole, demonstrating the relative position of tissue blocks used in the present sample (respectively corresponding to Brodmann areas 10 and 18). d = dorsal, l = lateral
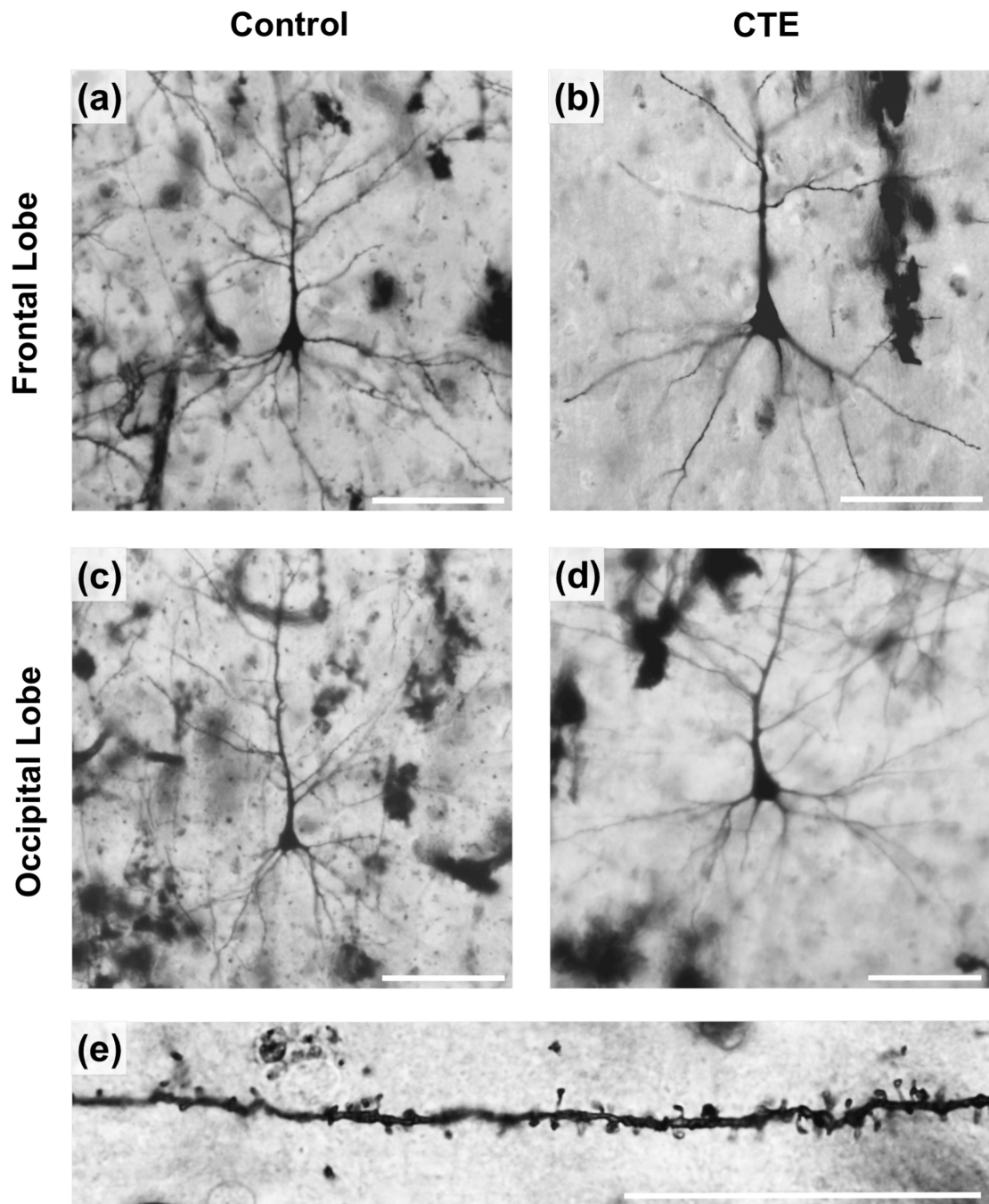
Control **CTE**

FIGURE 2.
The quality of the Golgi stain is illustrated in the photomicrographs of supragranular pyramidal neurons sampled from the frontal and occipital poles of the Control group (a,c) and chronic traumatic encephalopathy (CTE) group (b, d); basilar dendritic spines from a Control brain are also shown (e). For (a–d), scale bar = 100 μm. For (e), scale bar = 10 μm
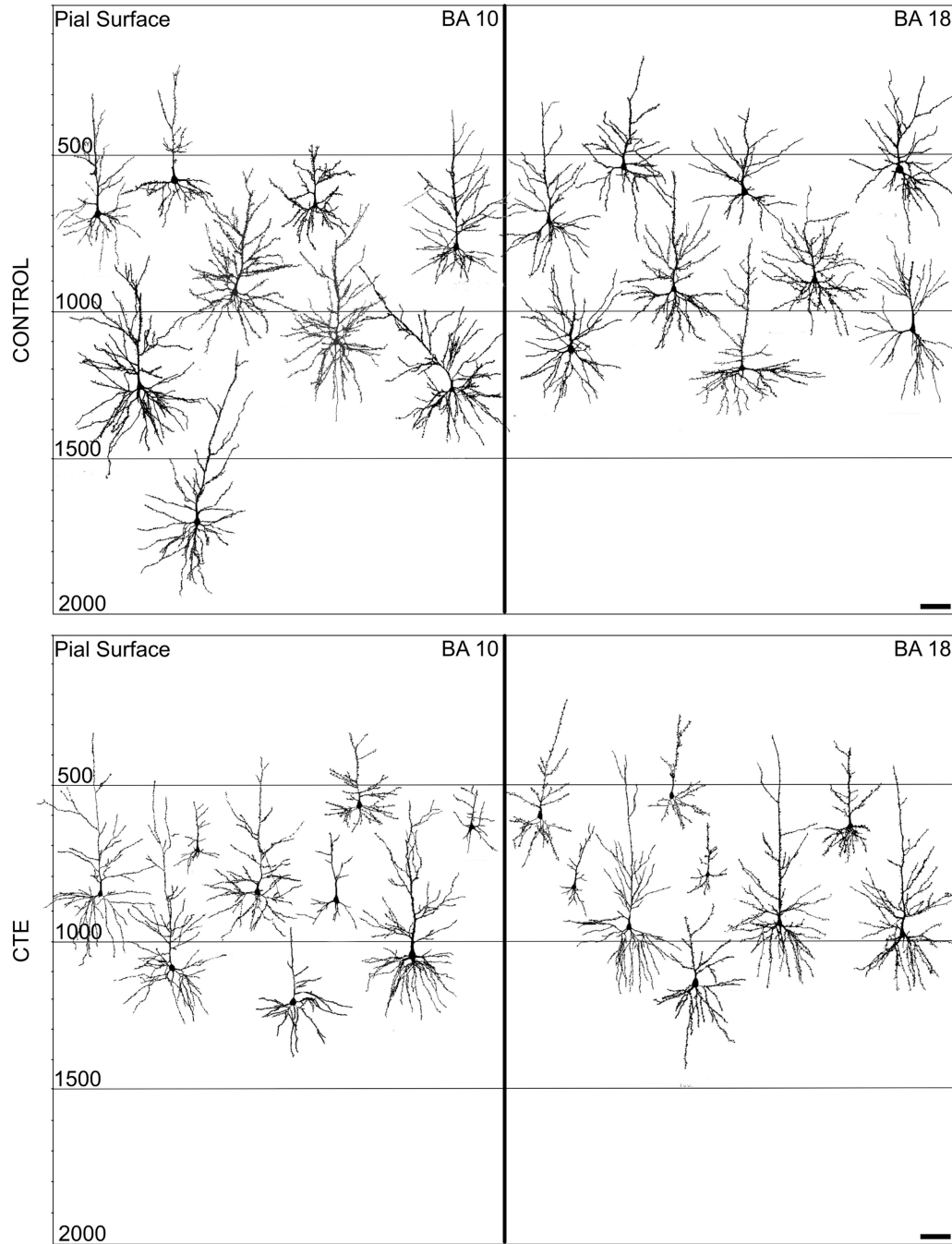
FIGURE 3.
Representative Neurolucida tracings of pyramidal neurons in the frontal (BA10) and occipital (BA18) poles from the Control and chronic traumatic encephalopathy (CTE) groups. Relative depth from the pial surface is indicated. Note the greater variability in dendritic extent for the CTE tracings compared to the Control tracings. Scale bars = 100 μm
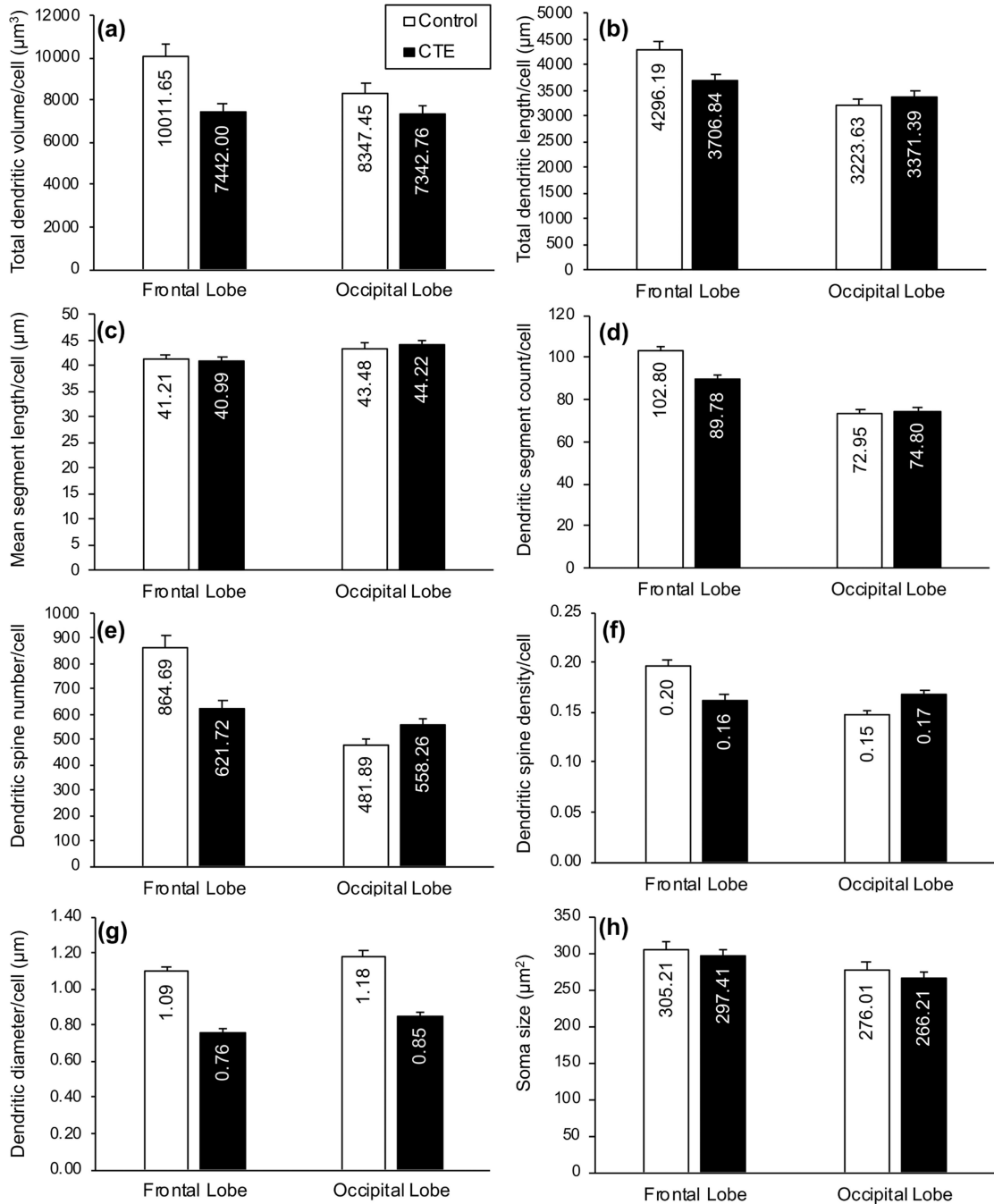
FIGURE 4.

Bar graphs showing differences in dendritic measures between groups (Control, chronic traumatic encephalopathy [CTE]): (a) total dendritic volume (Vol in μm^3); (b) total dendritic length (TDL, in μm); (c) mean segment length (MSL; in μm); (d) dendritic segment count (DSC); (e) dendritic spine number (DSN); (f) dendritic spine density (DSD; number of spines/μm of dendritic length); (g) dendritic diameter (Dia, in μm); and (h) soma size (in μm^2). In the Control group, with the exception of MSL, all dependent dendritic and spine measures appeared to be higher in the frontal lobe than the occipital lobe. Regional

differences in the CTE group were variable across measures. Between the two groups, Vol and Dia measures were lower in the CTE group than in the Control group for both regions, but TDL, DSC, DSN, and DSD were lower in the CTE group in the frontal lobe only. Only small differences in soma size between groups and regions were noted. Error bars represent *SEM*

FIGURE 5.

Bar graphs showing differences in dendritic measures between groups (Control, chronic traumatic encephalopathy [CTE]) and between dendritic trees (apical, basilar): (a) total dendritic volume (Vol in μm^3); (b) total dendritic length (TDL, in μm); (c) mean segment length (MSL; in μm); (d) dendritic segment count (DSC); (e) dendritic spine number (DSN); (f) dendritic spine density (DSD; number of spines/μm of dendritic length); and (g) dendritic diameter (Dia, in μm). Within-groups, basilar dendritic branches appeared to exhibit lower Vol and DSD, but higher TDL, DSC, and DSN, than apical branches.

Between-group differences generally reflected the patterns observed when both branch types were considered together. Error bars represent *SEM*
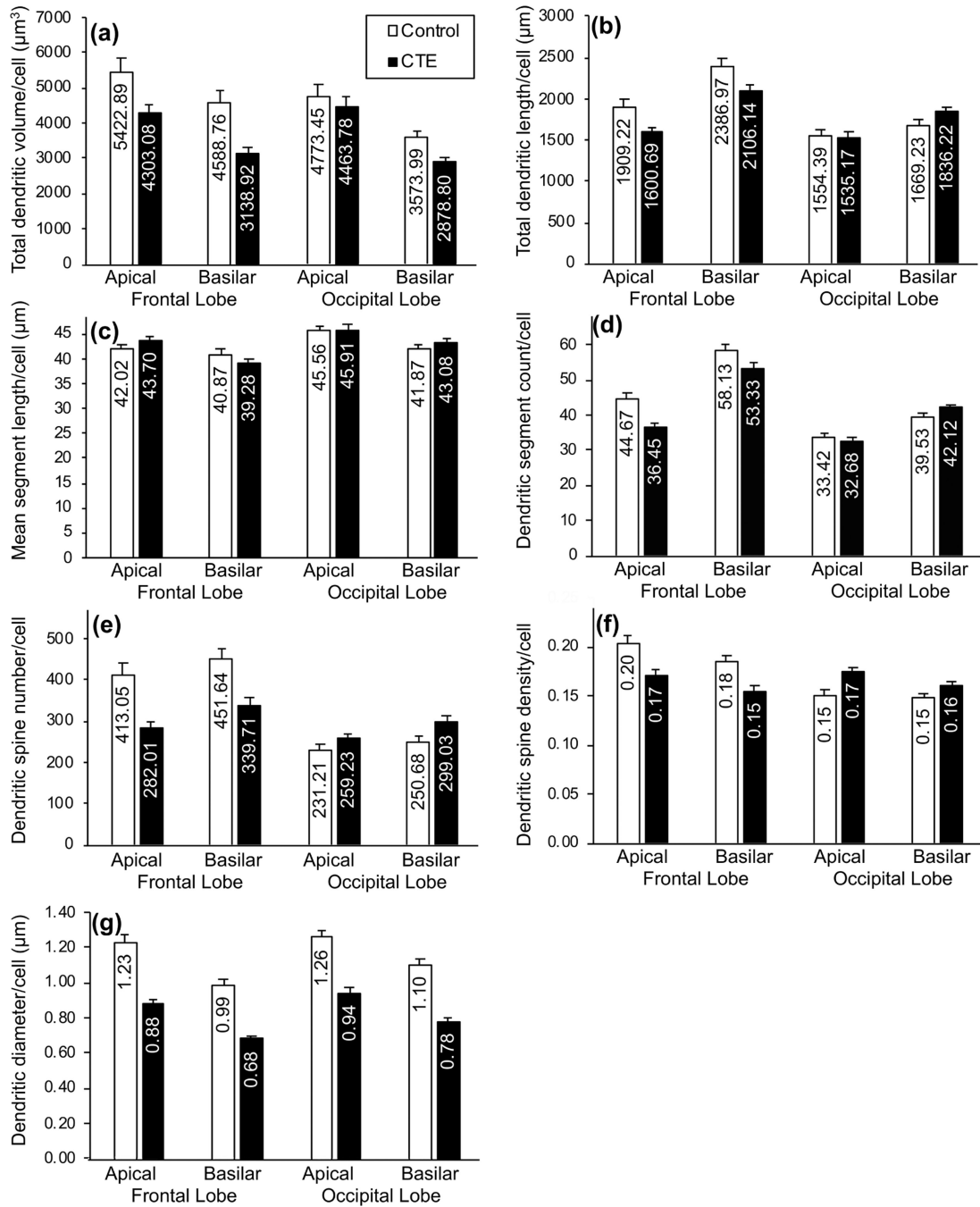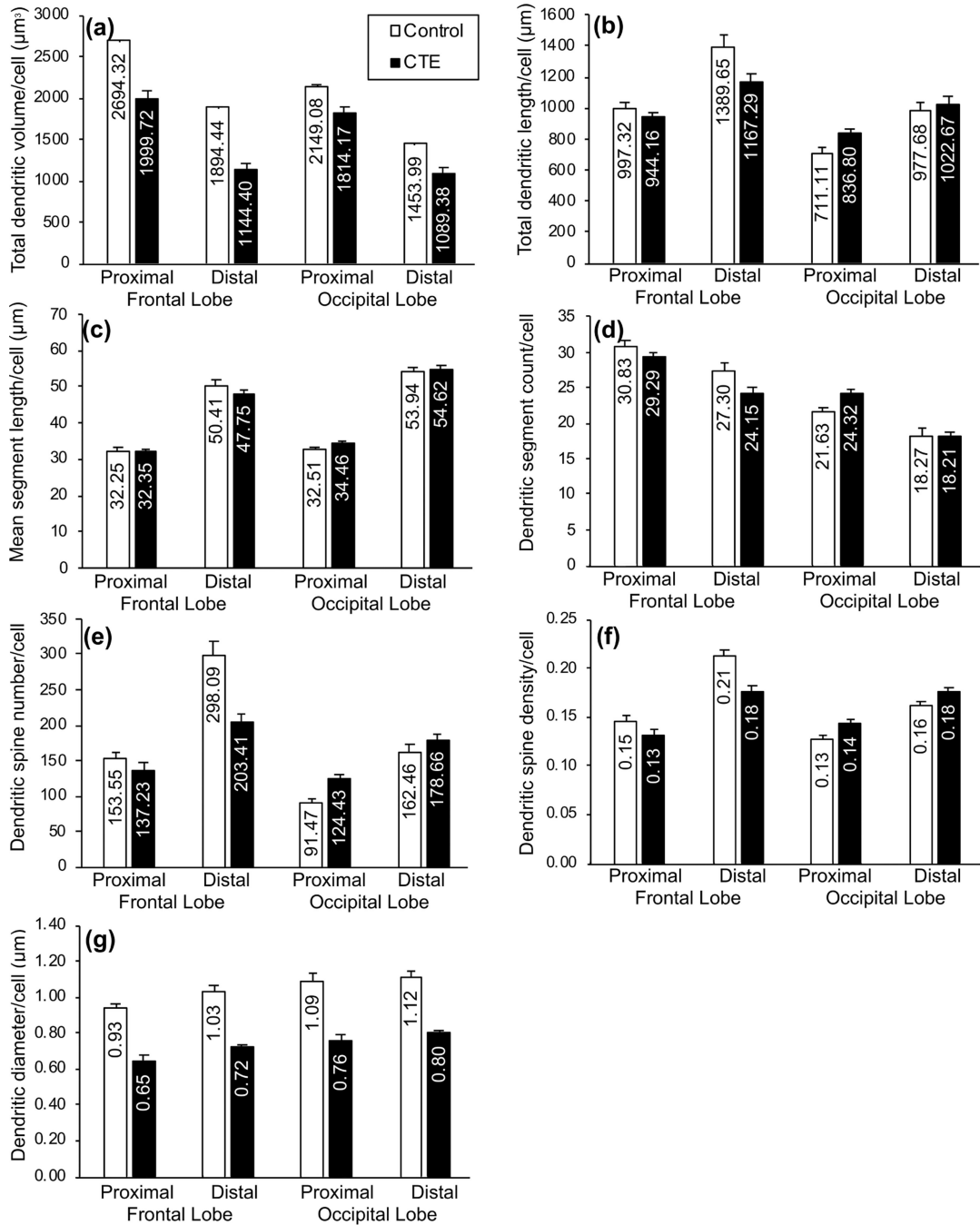
FIGURE 6.

Bar graphs showing differences in dendritic measures between groups (Control, chronic traumatic encephalopathy [CTE]) and between basilar dendritic segments (proximal, distal): (a) total dendritic volume (Vol; in μm^3); (b) total dendritic length (TDL, in μm); (c) mean segment length (MSL; in μm); (d) dendritic segment count (DSC); (e) dendritic spine number (DSN); (f) dendritic spine density (DSD; number of spines/μm of dendritic length); and (g) dendritic diameter (Dia, in μm). Within-groups, with the exception of DSC and Vol, proximal segment measures were lower than distal segment measures in both regions. In the

frontal lobe, between-group differences in Vol, TDL, DSC, DSN, and DSD were relatively greater in distal segments than in proximal segments. Discrepancies in proximal and distal measures between groups in the occipital lobe were not consistent across measures. Error bars represent *SEM*

(a)

(b)

(c)
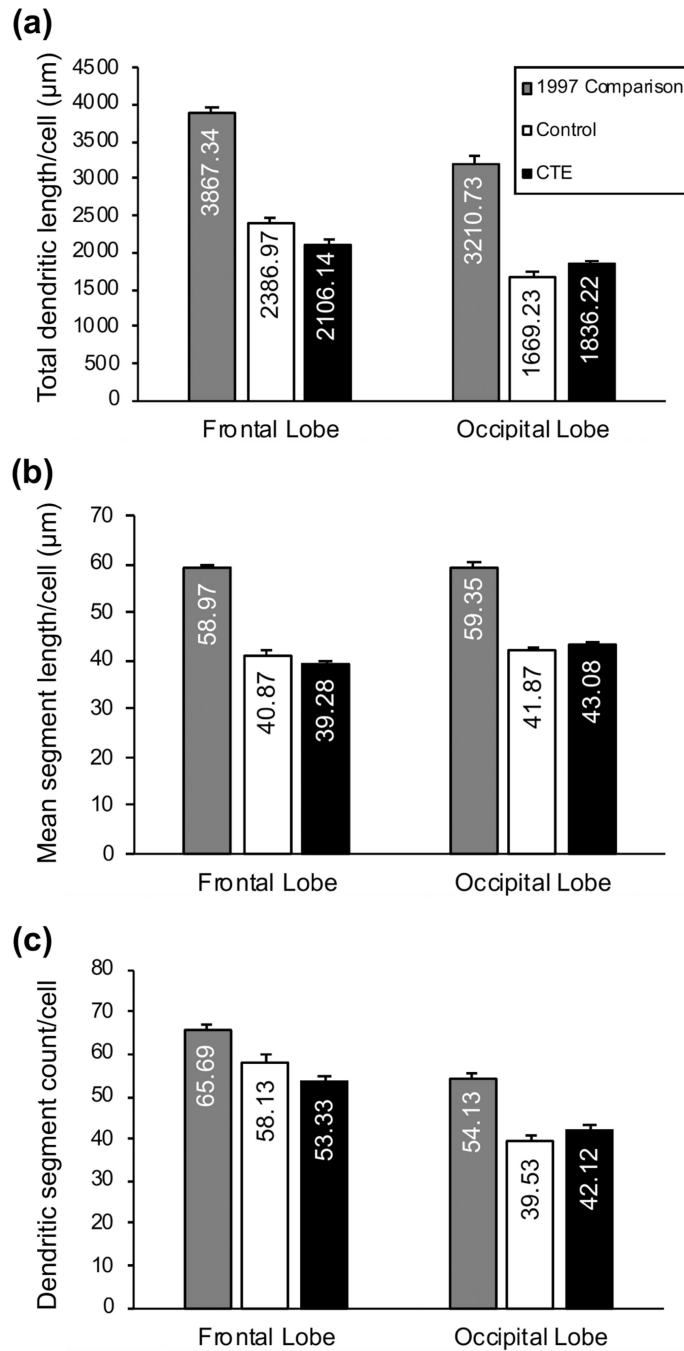
FIGURE 7.
Bar graphs of basilar dendritic measures in the 1997 Comparison group and the current Control and chronic traumatic encephalopathy (CTE) groups. (a) total dendritic length (TDL, in μm); (b) mean segment length (MSL; in μm); and (c) dendritic segment count (DSC). For all dependent measures, 1997 Comparison cohort values were larger than both current Control and CTE group values across both cortical regions. For the 1997 Comparison group, as in the Control group in the present study, dendritic extent was

consistently and descriptively greater in the frontal lobe than in the occipital lobe. Error bars represent *SEM*

TABLE 1

Case summaries

Subjects	AT (hrs)	FT (months)	Hemisphere	Cause of death	RHI	Years of play	CTE Stage	PreF. tau	Occip. tau	CERAD-NP score	TDP-43	Lewy body	AS	CAA
CTE														
M89	13.0	06.5	Left	Dementia	Hockey	58	I	1	1	2	N	Lim	++	+
M75	44.5	01.2	Right	Dementia	Football	17	III	1	1	3	Y	Olf	+	++
M70	15.0	08.5	Right	Glioblastoma	Football	24	III	1	0	0	Y	N	++	+
M78.1	23.0	10.0	Right	Dementia	Football	08	III	1	0	0	Y	Neo	++	+
M87.1	24.0	08.0	Left	Dementia	Football	16	III	1	0	1	N	N	+++	+
M87.2	29.0	01.1	Left	Dementia	Football	14	III	3	0	0	Y	N	+++	-
M67	48.0	03.2	Left	Dementia	Football	16	IV	3	2	1	Y	N	++	+
M73.1	41.0	08.0	Right	Dementia	Football	17	IV	3	0	1	Y	N	++	-
M85	26.5	07.0	Right	Myocardial infarction	Football	20	IV	2	0	1	Y	N	-	-
M77	36.5	03.3	Right	Dementia	Football	17	IV	3	0	1	Y	N	+++	+
M78.2	38.0	01.6	Left	Cardiac arrest	Football	08	IV	3	0	1	Y	Neo	+	+
Control														
M68	24.0	04.0	Left	Drowning	-	-	-	-	-	-	-	-	-	-
M71	19.4	23.0	Right	Cardiac arrest	-	-	-	-	-	-	-	-	-	-
M73.2	10.4	23.0	Right	Heart disease	-	-	-	-	-	-	-	-	-	-
M74	23.3	18.0	Right	Pulmonary embolism	-	-	-	-	-	-	-	-	-	-
F96	13.1	14.0	Right	Pulmonary embolism	-	-	-	-	-	-	-	-	-	-

Note: Subjects are referred to by sex (M = Male; F = Female) and by age in years. For example, M55 refers to a 55-year-old male. Cases with the same age have been arbitrarily differentiated with .1 or .2 designation. Note that CTE cases are arranged according to the severity of their CTE stage.

Abbreviations: AS, arteriosclerosis; AT, autolysis time; CAA, cerebral amyloid angiopathy; CERAD-PR, Consortium to Establish a Registry for Alzheimer's Disease neuropsychological assessment battery; CTE, chronic traumatic encephalopathy; FT, fixation time; RHI, repetitive head impact sport; PreF. tau, tau pathology score for the prefrontal cortex (scale = 0–3); Occip. tau, tau pathology score for the occipital lobe (scale = 0–3); TDP-43, presence of TDP-43 pathology (if yes, found in the amygdala, hippocampus, entorhinal/inferior temporal cortex and neocortex); Lewy Body, presence of Lewy body dementia (if yes, Lim, limbic; Olf, olfactory, Neo, neocortical): –, none, +, mild, ++, moderate, +++, severe.

TABLE 2

Variation within dendritic/spine measures

| Measure | Condition | Measures of central tendency | | Measures of distributional form | | | | | | t Test | |
		Mean	Median	Minimum	Maximum	Range	SD	Skew-ness	Kurtosis	t Statistic[a]	p Value[a]
Vol	Control	9,179.55	7,337.73	1,786.67	43,378.15	41,591.48	5,867.83	1.86	5.68	3.69	0.00
	CTE	7,392.29	5,665.56	1,301.00	38,999.85	37,698.85	5,598.12	2.08	5.91		
TDL	Control	3,759.91	3,615.60	1,255.92	9,732.41	8,476.49	1,574.87	1.00	1.74	Ns	
	CTE	3,539.11	3,202.72	937.94	9,922.06	8,984.12	1,648.13	0.90	0.56		
MSL	Control	42.35	41.29	22.48	70.62	48.14	9.75	0.37	-0.41	Ns	
	CTE	42.60	41.40	17.00	97.57	80.57	12.23	0.51	0.18		
DSC	Control	87.88	85.50	41.00	196.00	155.00	27.70	0.73	0.87	Ns	
	CTE	82.29	77.00	26.00	214.00	188.00	28.05	0.92	1.09		
DSN	Control	673.29	558.50	150.00	2,911.00	2,761.00	424.40	1.68	4.62	Ns	
	CTE	589.99	500.50	47.00	2,266.00	2,219.00	405.55	1.53	2.97		
DSD	Control	0.17	0.17	0.07	0.34	0.27	0.06	0.60	0.02	Ns	
	CTE	0.16	0.15	0.03	0.46	0.43	0.08	1.12	1.65		
Dia	Control	1.13	1.10	0.48	1.99	1.51	0.32	0.35	-0.52	Ns	
	CTE	0.80	0.73	0.23	1.93	1.70	0.35	0.57	-0.43		
Soma size	Control	290.61	275.00	78.00	655.00	577.00	110.43	0.72	0.35	Ns	
	CTE	281.81	263.35	70.60	878.70	808.10	113.42	1.15	2.55		

Note: Although Control values are greater than CTE values for most attributes (52 of 64 comparisons), results indicate minimal differences in mean and median values between Control ($N = 200$) and CTE ($N = 440$) neurons. Bold values show between-group differences >50% (8 of 64 comparisons); italic values are where the CTE values were less extreme than Control values (12 of 64 comparisons).

Abbreviations: CTE, chronic traumatic encephalopathy; Dia, dendritic diameter; DSC, dendritic segment count; DSD, dendritic spine density; DSN, dendritic spine number; MSL, mean segment length; TDL, total dendritic length; Vol, dendritic volume; Ns, not significant.

[a] t and p Values are used to exemplify the slight variation in means over dendritic measures (with Scheffé corrections for multiple tests). Unlike the MARSplines analysis, they do not adequately account for the multiply dependent nature of the data or non-normal distribution of some attributes.